RSC Advances

ROYAL SOCIETY OF CHEMISTRY

www.rsc.org/advances

Development of polybenzoxazine/TSBA-15 composite from renewable resource cardanol for low k applications

V.Selvaraj[a]*, K.P. Jayanthi[a,b], T.Lakshmikandhan[c] and M.Alagar[c]

[a]Nanotech Research Lab, Department of Chemistry, University College of Engineering Villupuram, (A Constituent College of Anna University, Chennai), Kakuppam, Villupuram-605 103, Tamilnadu, India.

[b]Department of Chemistry, D.M.I College of Engineering, Palanchur-Nazarethpet Post, Chennai-600123.

[c]Polymer Composite Lab, Department of Chemical Engineering, Anna University, Chennai-600 025, India.

Abstract

The present work describes the synthesis of a novel cardanol based benzoxazine monomer (CBz) from renewable resource of cardanol using caprolactamdiamine (CPLDA) by a solventless method. Thiol functionalized mesoporous silica (TSBA-15) was incorporated into cardanol based benzoxazine matrix (PCBz) and the structure of TSBA-15/PCBz was confirmed by FT-IR and NMR analysis. Surface morphology of TSBA-15/PCBz was determined by SEM and TEM techniques. From the TEM results, it was observed that the dispersion of thiol functionalized mesoporous silica in to PCBz forms a fibrous material, which imparts free volume. Thermal properties were studied by DSC and TGA analysis. From the results, it was noticed that the enhanced thermal properties were observed with varying the weight percentage of TSBA-15 material. Dielectric data obtained from impedance analyzer shows that the TSBA-15/PCBz composites have lower values of dielectric constant, and dielectric loss. These above results conclude that TSBA-15/PCBz composites obtained from a renewable waste cardanol finds application as electrical resistance material in microelectronic applications.

Key words: Cardanol, TSBA-15, Low -k, Polybenzoxazine, Microelectronics applications.

*Corresponding Author: V. Selvaraj, E.mail: rajselva_77@yahoo.co.in (V.Selvaraj), Fax: 04146-224500

Introduction

Inorganic materials which are traditionally used as dielectrics are brittle and consume high energy for processing even though they possesses several superior qualities such as excellent thermal, dielectric and magnetic properties [1]. Polymers, on the other hand are flexible with high resistivity and better processibility show low thermal and dielectric properties. Combining these two materials in the form of polymer hybrid composites could lead to the development of a new type of materials with improved performance for dielectrics and electrical insulation properties. Both materials with low and high dielectric constant (k) are essential in electronic industries. Low dielectric constant is required basically as insulators. The applications of these passivation materials ranged in isolating signal-carrying conductors from each other, fast signal propagation, interlayer dielectric to reduce the resistance-capacitance (RC) time delays, crosstalk and power dissipation in the high density and high speed integration [2]. In advanced integrated circuit (IC) chips, polymers such as polyimides, polybenzoxazine, polyarylethers, fluoropolymers, and polysilsesquioxanes, etc. have been employed as potentially low k materials [3,4]. Among the polymeric dielectrics, polybenzoxazines are relatively new class of novel thermoset polymeric materials that are formed by thermally activated ring opening polymerization without any catalyst and generating no byproducts [5, 6].

Polybenzoxazines exhibit unique properties like nearly zero shrinkage upon curing, good thermal stability, good chemical resistance, low water absorption and wide processing window [7-11]. Though the dielectric constants of polybenzoxazines are low, it needs to be reduced further to find better utility in microelectronics applications. Different approaches have been made to reduce the dielectric constant of polybenzoxazine like the incorporation of a fluorinated substituent into skeleton of polybenzoxazine [12], nano-porous poly (caprolactone–cobenzoxazine) [13] and introduction of an air gap into the interconnected structures by blending with nanoporous materials [14-16]. The dielectric constant can be reduced by embedding air voids into the polymer matrix [17, 18] which has a dielectric constant of one. The mesoporous silica nanofillers have received much attention due to their ordered structure, high surface area and easiness for functionalization of the nanopores. The nanopores are sufficiently porous to accommodate macromolecules, which will lead to intimate interactions between the polymer and the inorganic phase [19].

Generally benzoxazines are synthesized from petrochemicals, which is a depleting resource. Several research groups have reported the synthesis of benzoxazine monomers using renewable resources [20-22]. To the best of our knowledge, there is no report on the preparation of a novel dielectric material from an agrochemical renewable resource cardanol using caprolactamdiamine by solventless method. A novel attempt was made to improve the properties of polybenzoxazine using cardanol as renewable resource. Further the present work investigates the influence of thiol functionalized mesoporous silica SBA-15 on the thermal and dielectric properties by varying the weight percentage of TSBA-15. In order to get a well-dispersed composite with enhanced interfacial adhesion, surface of the nanoparticles are modified with MPTMS. Thus the prepared TSBA-15/polybenzoxazine nanocomposite is expected to have flexibility along with low dielectric characteristics.

Experimental

Materials

Cardanol was procured from Satya Cashew Chemicals Pvt.Ltd. Chennai, (India), Paraformaldehyde, 6-aminocaproic acid, 4,4’-methylene dianiline and N-Methylpyrrolidone (NMP) were obtained from Sigma-Aldrich.

Synthesis of Caprolactam Diamine (CPLDA)

Caprolactam based diamine (CPLDA) was synthesized by using caprolactam, 4, 4’ diaminodiphenylmethane, NMP and alkali hypo phosphate as a catalyst. In a 250ml two-necked round-bottomed flask equipped with a condenser, 100 ml NMP, 10 g (0.0883mol) of caprolactam, 7.8 g (0.0442mol) of 4, 4’ diaminodiphenylmethane and 5 mg of alkali hypo phosphate catalyst were added. The above reaction mixture was allowed to react at 160 ^{o}C for 24 h with efficient agitation to facilitate completion of reaction. The resulted product was filtered as solid material with the yield of 85% **(Scheme 1).**

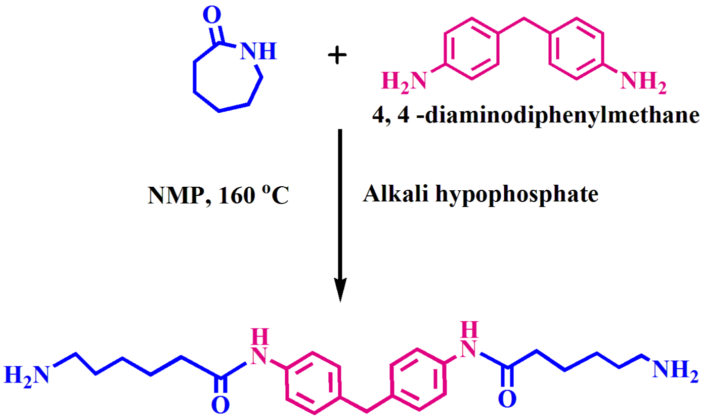

Scheme 1 Synthesis of N,N-(4,4-methylene bis(4,1-phenylene))bis(6-aminohexamine) (CPLDA)

Synthesis of cardanol benzoxazine monomer(CBz)

The cardanol based benzoxazine monomer was synthesized by using a single step condensation reaction of aromatic caprolactamdiamine (CPLDA), cardanol and paraformaldehyde by following a solventless method [23]. A mixture of cardanol (6.59 g, 0.022 mol), paraformaldehyde (1.39 g, 0.046mol), and CPLDA (5g, 0.011mol) were taken in a 500ml three neck round-bottom flask equipped with a magnetic stirrer, and refluxing condenser. The reaction mixture was refluxed at 85°C for 1h and at 130°C for another 5h. Then the reaction mixture was allowed to attain the room temperature. To the above reaction mixture, chloroform (100 mL) was added and organic layer was washed with aqueous sodium hydroxide (2 N) followed by distilled water. The organic layers were combined, dried over sodium sulphate and filtered to give red oil. The solvent was removed under reduced pressure and the residue was dried at 353 K under vacuum to give benzoxazine (CBz) as brown viscous solid (**Scheme 2**). ^{1}H-NMR (300 MHz,$CDCl_3$): 0.86–0.93 (t, -CH_3,6H(a)), 1.2–1.3 (m, -CH_2, 20H(b)), 1.4–1.86 (m, -CH_2CH= 8H(c)), 1.96-2.25(-CH_2-CO(d)), 2.6(t, -CH_2-N-(e)), 2.8-3.0(t, CH_2Ar(f)) , 6H, 3.2(s, Ar-CH_2-Ar(g)), 3.8 (s, ArCH_2N–(h)), 4.6(s, O-CH_2-N-(j)) 5.20–5.50(m, -CH=CH-(k)), 6.63–6.80 (Ar-H, 6H(l), 6.9–7.40 (Ar-H, m (m,n) 6.90 (-N-H (p)). FTIR (KBr disc): 3008, 2950, 2848, 1620, 1247, 1172, 1100 and 960 cm^{-1}. MALDI Mass: m/e = 1075.6.

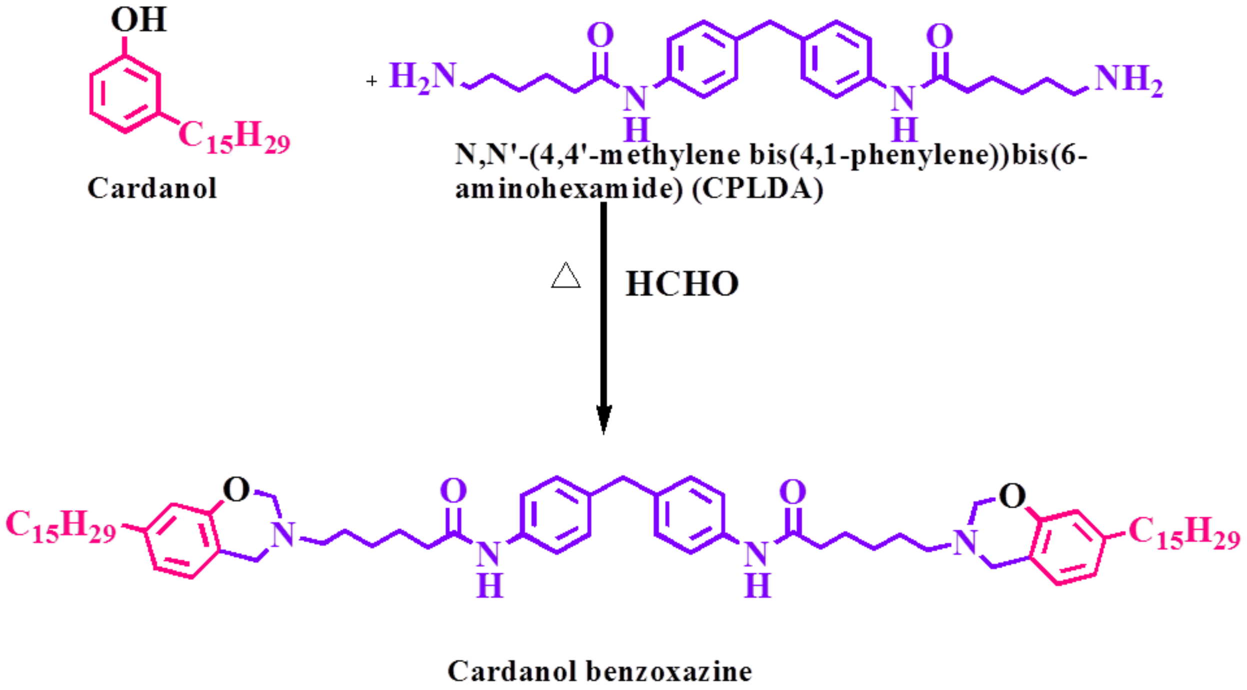

Scheme 2 Synthesis of Cardanol Benzoxazine (CBz)

Synthesis of SBA-15

About 4 g pluronic polymer was dissolved in 150 ml of 1.6 M HCl (pH<2). After heating the above reaction mixture to 40ºC, 0.3 g of TMB (swelling agent) and 9.2 ml of TEOS (inorganic precursor) were added under vigorous stirring condition. The reaction mixture was then transferred into a tightly sealed Teflon bottle. The bottle was aged at 80^{o}C for 24 h. After 24 h, the mixture was cooled, and then filtered by vacuum filtration to get a white powder sample. The white powder was allowed to dry in an air under vacuum for 24 h. The dried sample was calcinated in air at 550^{o}C for 6 h with a heating rate 1^{o}C/min. The final mesoporous product designated as SBA-15 was obtained.

Preparation of thiol functionalized SBA-15 (TSBA-15)

Thiol functionalized SBA-15 (TSBA-15) was synthesized as per the reported procedure [24]. Mesoporous silica was dispersed in ethanol under ultrasonic agitation for 30 min, and then the calculated amount of MPTMS was added to the above reaction mixture, and refluxed for 24 h under vigorous stirring. Finally the reaction mixture was filtered and the obtained product was washed with ethanol followed by hexane in order to remove the unreacted MPTMS and then dried in the vacuum oven at 50^{o}C for 24 h.

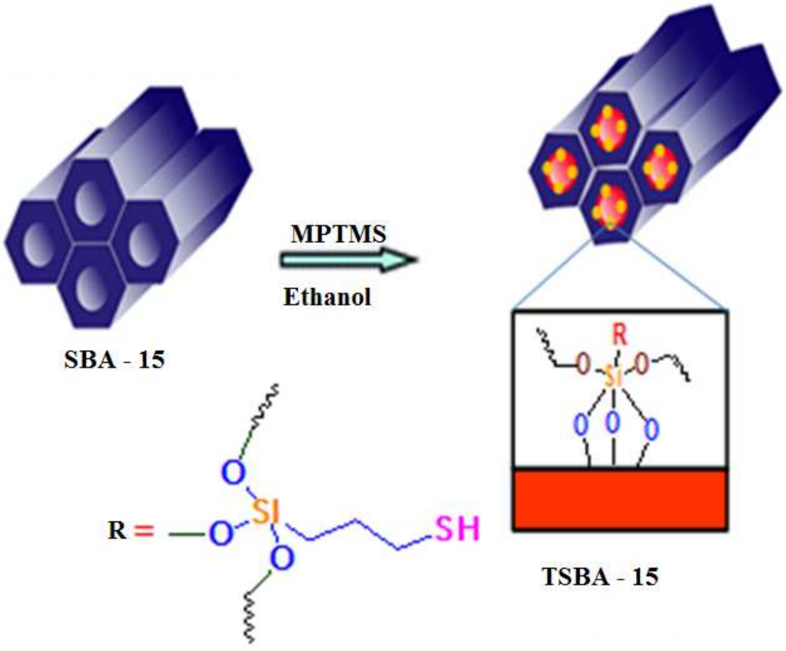

Scheme 3 Synthesis of thiol functionalized SBA-15 (TSBA-15)

Preparation of polybenzoxazine (PCBz)

The monomer CBz was dissolved in $CHCl_3$ and the solution was poured in a silane coated glass plate, which was cured at 120^0C for 1 h, 160^0C for 1 h, 180^0C for1 h, 200^0C for 2 h, and 220^0 C for 2 h to get a transparent film for comparative studies.

Preparation of cardanol based polybenzoxazine (PCBz)/TSBA-15 hybrid composites

Cardanol based polybenzoxazine/TSBA-15 hybrid films were synthesized according to the following **Scheme 4**. About 2 g of benzoxazine monomer was dissolved in 5 ml $CHCl_3$. Varying weight percentages of TSBA-15 (1%, 3% and 5%) dissolved in $CHCl_3$ were added gradually to the benzoxazine monomer solution and sonicated for 1h. The solution was poured in a silane coated glass plate and then cured at 120^0C for 1 h, 160^0C for 1 h, 180^0C for 1 h, 200^0C for 2 h, and 220^0 C for 2 h in order to get a semi transparent films (**Scheme 4**).

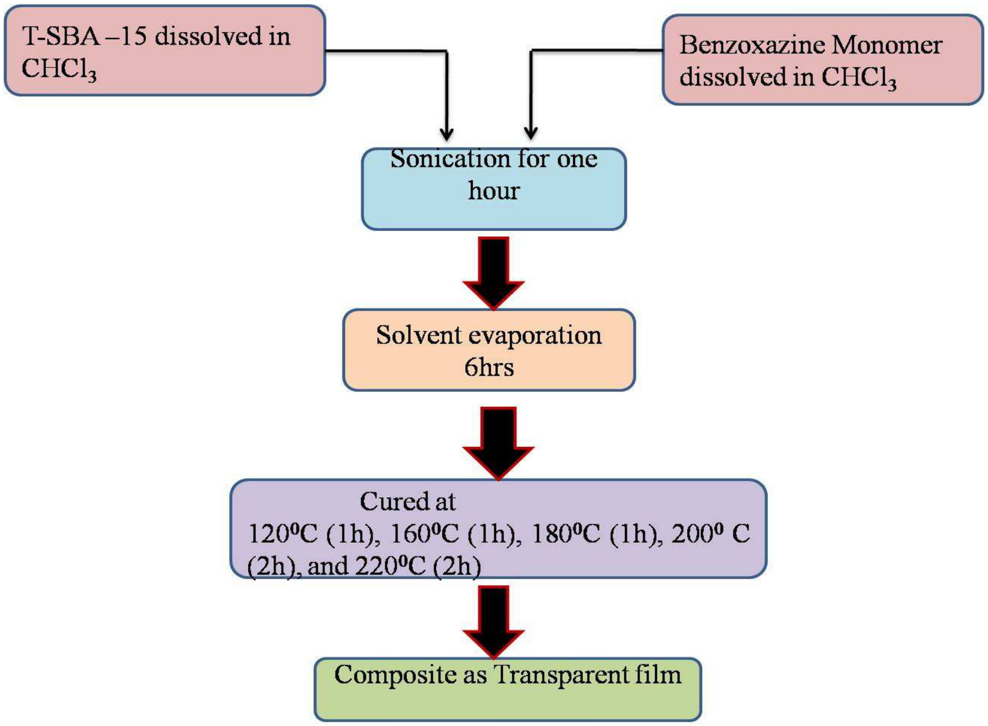

Scheme 4 Preparation of TSBA-15/PCBz hybrid composites

Characterization techniques

FT-IR spectra were recorded on KBr disc with a Perkin Elmer 6X FT IR spectrometer. ^{1}H NMR spectra was carried out on a Bruker 300 spectrometer using CDCl$_3$ as solvent. A Netzsch DSC-200 differential scanning calorimeter was used for the calorimetric analysis at a heating rate of 10^{0}C/min under continuous flow of nitrogen. Thermo-gravimetric analysis was performed in a DSC-2920 coupled with a TA-2000 control system at a scanning rate of 10^{0}C/min under nitrogen atmosphere. The dielectric constant (DC) of PCBz/ TSBA-15 systems were determined with the help of an impedance analyzer (Solartron impedance/gain phase analyzer 1260) using Pt electrode at 40^{0}C in a frequency range of 1MHz. Powder X-ray diffraction patterns (XRD) were recorded using a Rigaku Mini flex diffractometer with Cu-KR radiation. A JEOL JSM-6360 field emission scanning electron microscope was used for morphological studies. The phase morphology of PBCz/TSBA-15 nanocomposites was characterized by using a HR-TEM (JEM-3010, JEOL, Tokyo, Japan), operating at 80 kV with a measured point-to-point resolution of 0.23 nm.

Result and Discussion

FTIR studies

Figure 1 shows the FTIR spectrum of caprolactamdiamine (CPLDA). The characteristic absorption peak appeared at 1510 cm^{-1} indicates the existence of aromatic C= C and the presence of NH_2 was confirmed by the peak observed at 3400 cm^{-1}. The absorption peak visualized at 2925cm^{-1} and 2852 cm^{-1} indicates C–H aliphatic stretching vibration and the peak at 1660 cm^{-1} indicates the presence of C=O stretching of amide linked amine group present in the CPLDA.

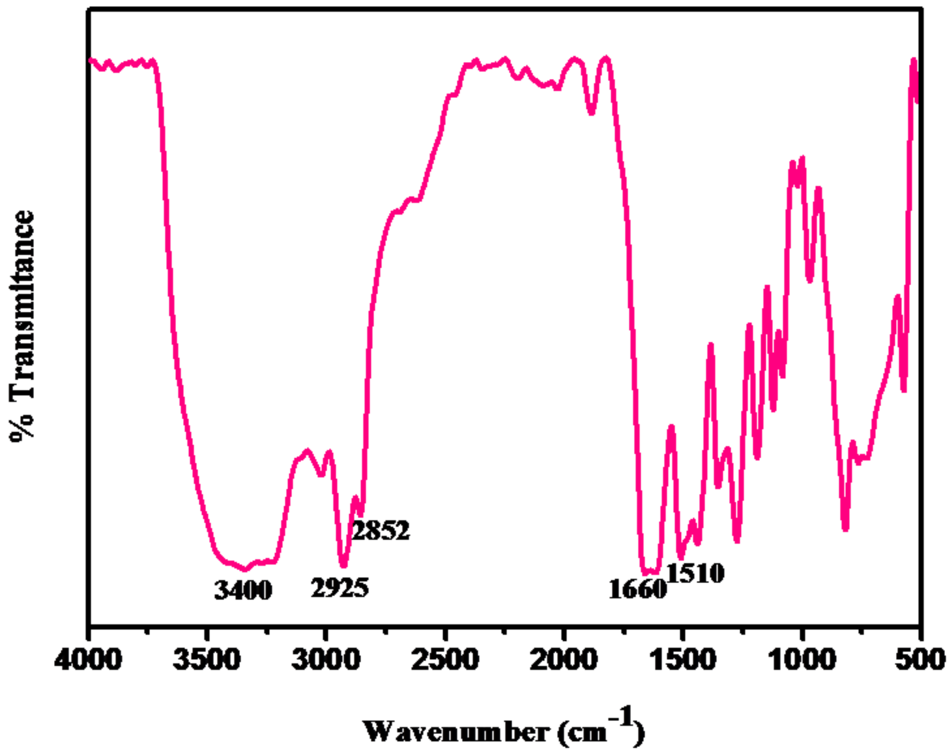

Figure 1 FTIR spectrum of caprolactamdiamine (CPLDA)

The molecular structure of cardanol benzoxazine (CBz) monomer was confirmed by FTIR spectrum (Figure 2).

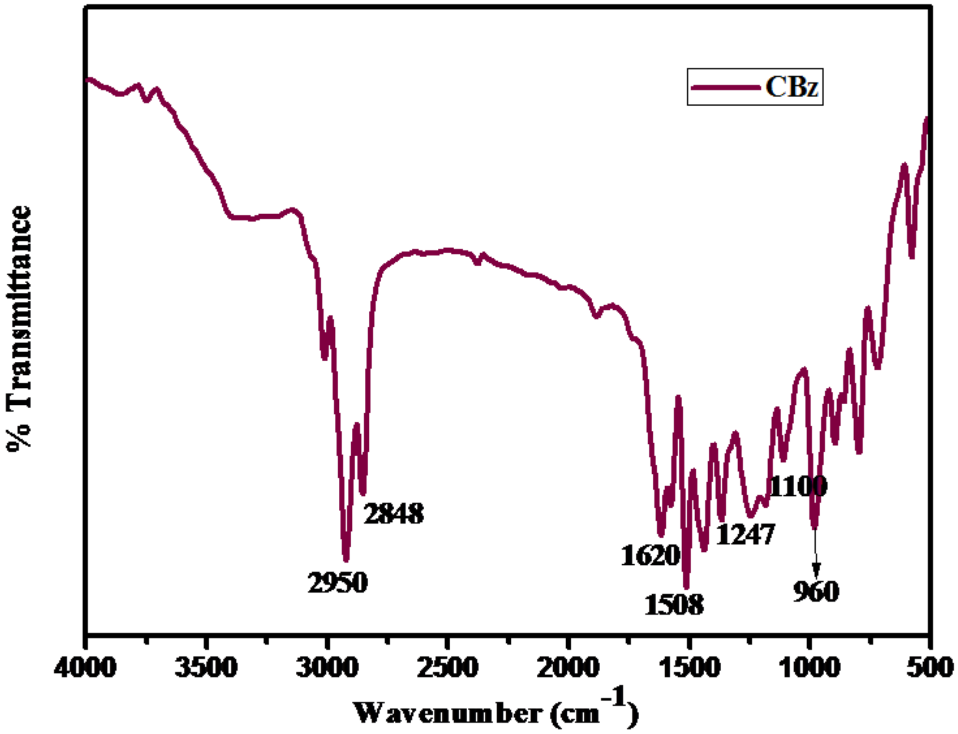

Figure 2 FTIR spectrum of cardanol benzoxazine (CBz)

The characteristic absorptions peaks appeared at 1247 cm^{-1} and 1172 cm^{-1} were assigned to asymmetric stretching of Ar-O-C, and symmetric stretching of C-O-C in cardanol benzoxazine (Figure 2), respectively. The peaks appeared at 2950 cm^{-1} and 2848 cm^{-1} were corresponding to C–H aliphatic stretch vibration. The peaks observed at 1620 cm^{-1} and 1508 cm^{-1} confirm the presence of 1,2,3-trisubstituted benzene ring in cardanol benzoxazine. Further, N–C–O stretching and Ar–O–C symmetric stretching vibrations were appeared at 960 cm^{-1} and 1100 cm^{-1}, respectively.

In the IR spectrum of TSBA-15, the appearance of an absorption peak at 2565 cm^{-1} confirms the presence of –SH group in functionalized mesoporous silica [Figure 3]**.** The strong bands at 2925-2854 cm^{-1} and 1437 cm^{-1} were attributable to C-H stretching and bending vibrations, respectively. In addition, the typical Si-O-Si bands were obtained at around 1100 cm^{-1} and 807 cm^{-1} confirm the formation of a condensed silica network.

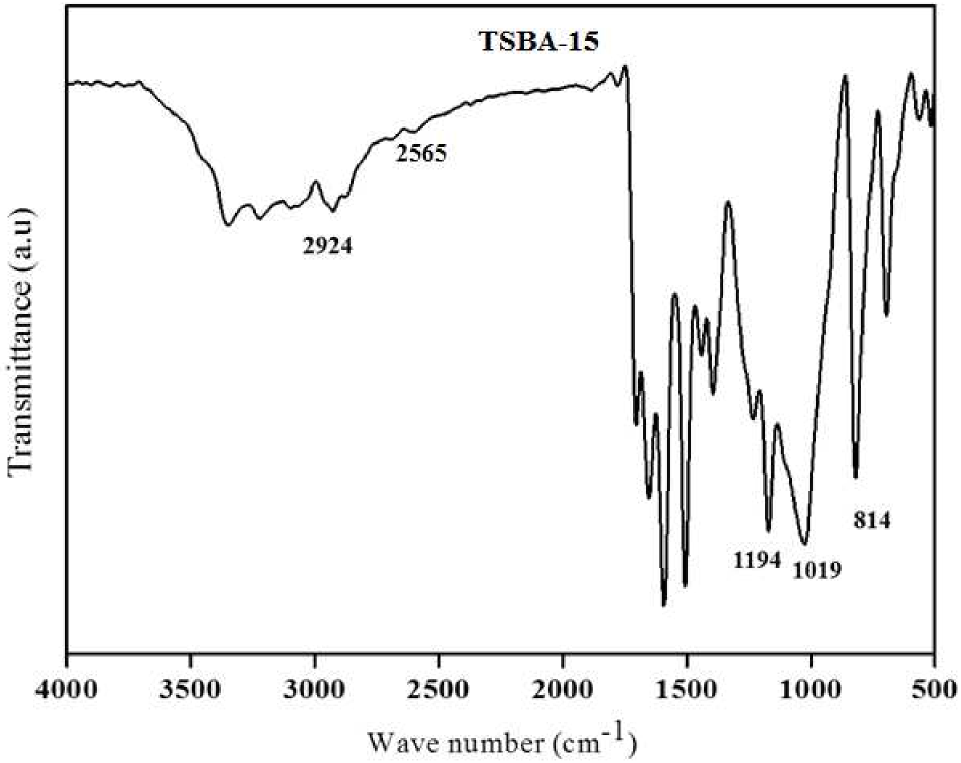

Figure 3 shows the FTIR spectrum of thiol functionalized SBA-15 material

The curing reaction of CBz and its composite with TSBA-15 were further confirmed by FTIR analysis. Figure 4 shows the FTIR spectra of PCBz and its composite with TSBA-15 material.

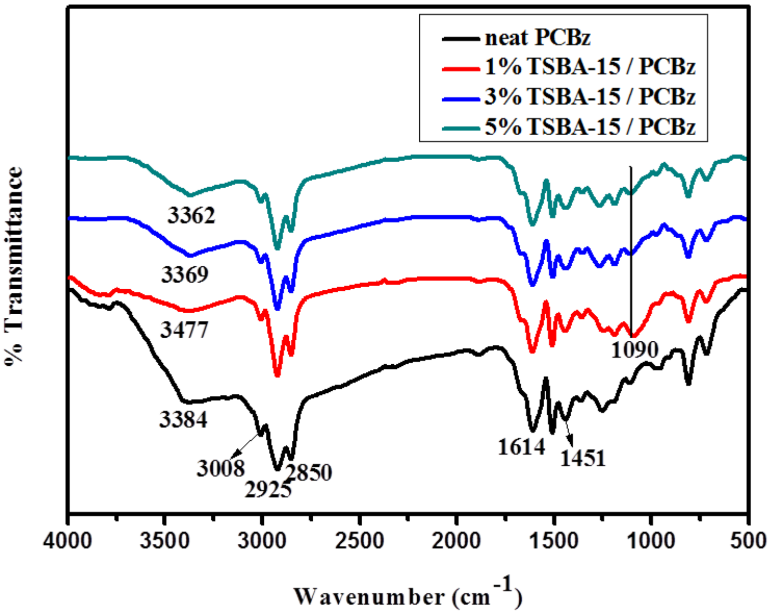

Figure 4 FTIR spectra of PCBz and TSBA-15/PCBz composites

Polybenzoxazine (PCBz) as well as TSBA-15 reinforced PCBz composites show a new absorption peak at 1451 cm^{-1} is due to the presence of tetra substituted benzene ring (Figure 4), which confirms the ring-opening polymerization of CBz (5–8). However, such a peak was not found in the case of CBz monomer (Figure 2). The absorption peaks appeared at 2925 cm^{-1} and 2850 cm^{-1}confirm the presence of C–H aliphatic groups. The absorption peak observed at 3008 cm^{-1} represents the aromatic C–H stretching. The absorption peak appeared at 1614 cm^{-1} corresponds to aliphatic C = C stretching frequency. In addition, the absorption peak visualized at 1090 cm^{-1} confirms the formation of –Si–O–Si–linkage due to the occurrence of hydrolysis of TEOS followed by condensation reactions of resulting Si-OH. The broad absorption peak appeared at 3384 cm^{-1} corresponds to vibration of O–H linkage of phenolic group present in PCBz. It was also noticed that the shift and broadening of this peak in the cases of TSBA-15 reinforced PCBz composites with 1, 3 and 5 wt % of TSBA-15 were observed at 3377 cm^{-1}, 3369 cm^{-1} and 3362 cm^{-1} respectively. It is also explained that the shift and broadening of peak occurred due to (Figure 4) the existence of hydrogen bonding interactions between TSBA-15 and cardanol. The presence of thiol group in mesoporous silica was confirmed by the absorption peak at 2565 cm^{-1} in the IR spectrum of TSBA-15 (Figure 3). However in the IR spectra of TSBA-15 incorporated PCBz composites, the peak at 2565 cm^{-1} is totally invisible or disappeared, due to chemical interaction between S-H groups and PCBz (Figure 4) [25, 26].

NMR spectrum of caprolactamdiamine (CPLDA)

The structure of caprolactamdiamine (CPLDA) was confirmed by ^{1}H NMR. Figure 5 shows the NMR spectrum of CPLDA.

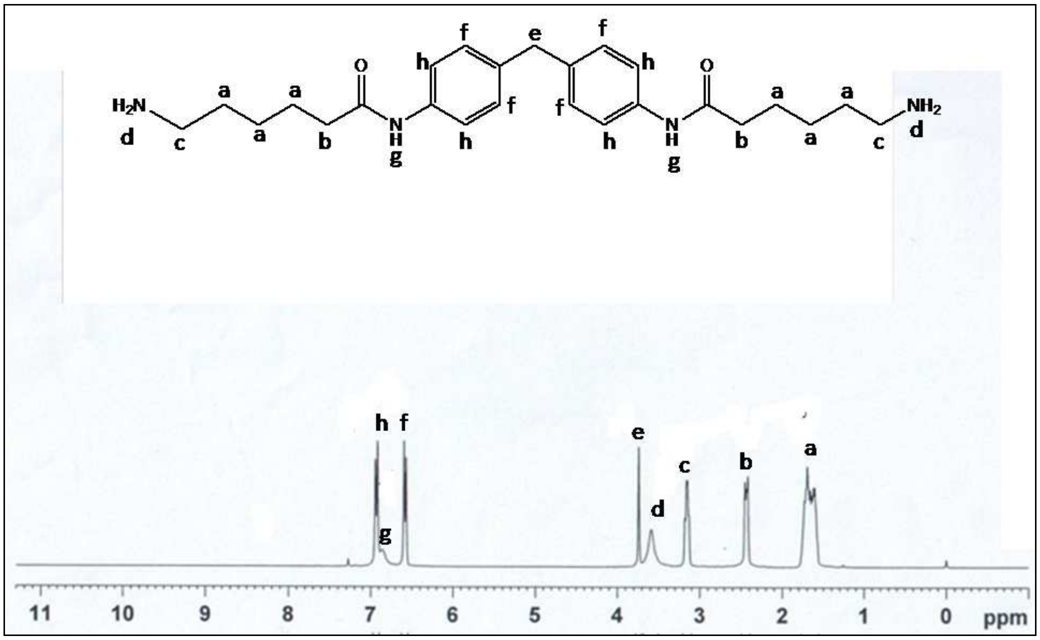

Figure 5 ^{1}H NMR spectrum of caprolactamdiamine(CPLDA)

The peak appeared at 3.13-3.30 ppm (c) was assigned to methylene (-CH$_2$-NH$_2$-) protons. The peaks at 6.59 ppm (f) and 6.94 ppm (h) were assigned to aromatic protons. Further, the peaks appeared at 1.62 ppm (a), 2.42 ppm (b) and 3.8 ppm (e) were correspondng to aliphatic protons and the peak at 3.59 ppm (d) was assigned to –NH$_{2.}$. Thus, the ^{1}H NMR study confirms the formation of caprolactamdiamine**.**

NMR and MALDI Mass spectra of cardanol benzoxazine (CBz)

The molecular structure of the monomer (CBz) was confirmed by ^{1}H NMR, ^{13}C NMR and MALDI mass techniques, which were shown in Figures 6, 6a and 6b.

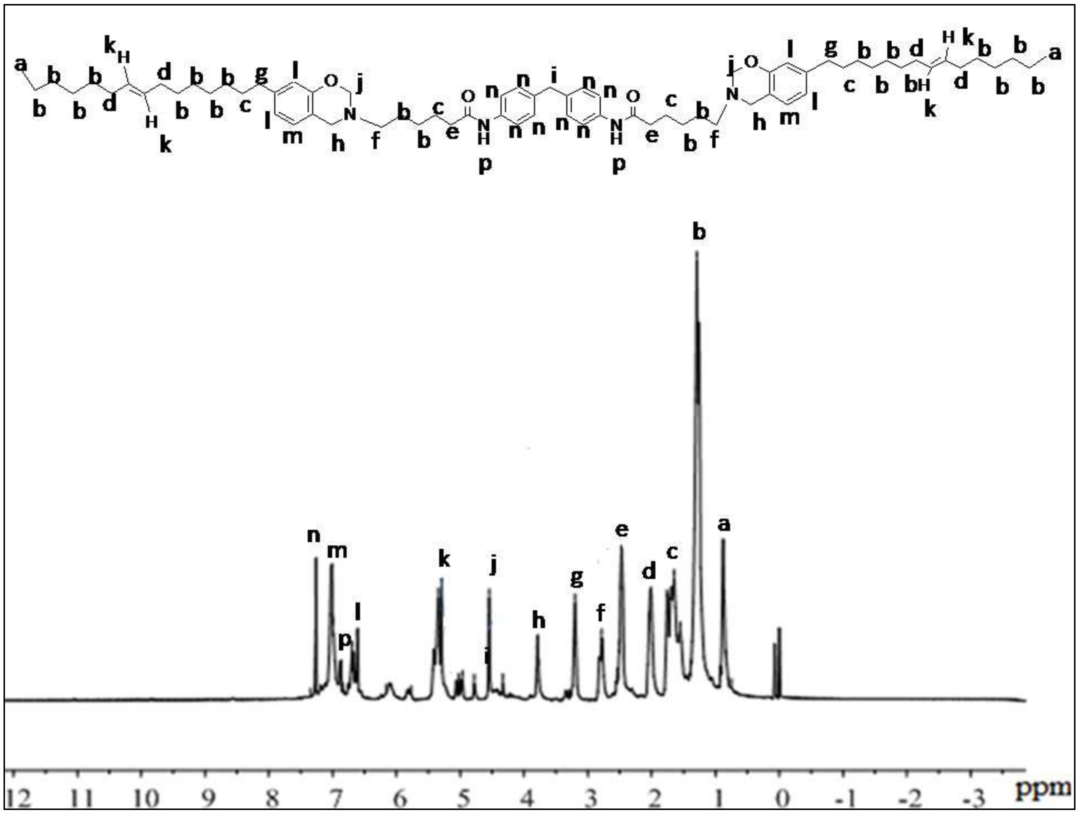

Figure 6 ^{1}H NMR spectrum of cardanol benzoxazine (CBz)

The characteristic protons of oxazine ring appeared at 4.6 ppm was assigned to O-CH$_2$-N- and the peak at 3.8 ppm was corresponding to Ar-CH$_2$-N-. The peaks observed from 6.63 to 7.40 ppm were assigned to methylene protons attached to aromatic hydrogens. This evidences that the hydroxyl functional group of cardanol was involed in the formation of oxazine ring structure and hence ascertains the successful formation of CBz monomer. The peak appeared at 5.51 ppm was ascertained to -CH=CH- originally present in the long alkyl side chain of cardanol monomer. The above results suggest that the formation of oxazine ring structure and hence successful formation of cardanol-based benzoxazine monomer.

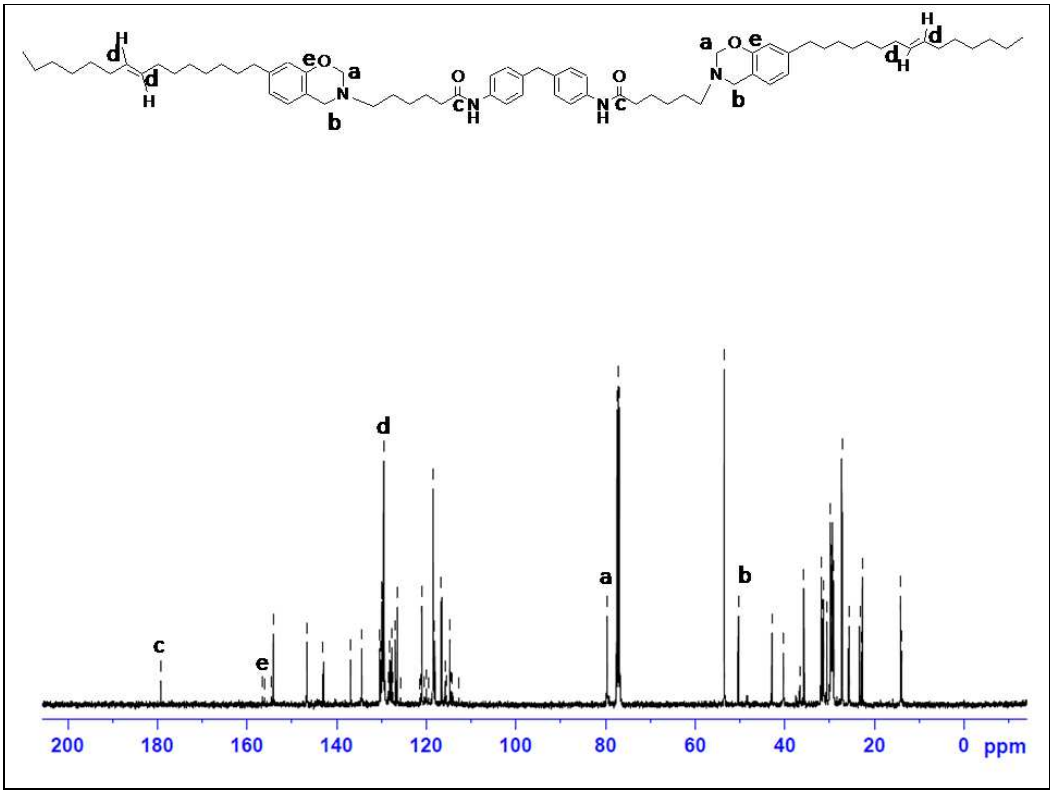

Figure 6a ^{13}C NMR spectrum of cardanol benzoxazine (CBz)

Further, cardanol-based benzoxazine monomer formation is confirmed by ^{13}C NMR spectrum (Figure 6a). The appeared peak at 80 ppm was assigned to – O-CH$_2$-N carbon and the appearance peak at 52 ppm shows the presence of ph-CH$_2$-N carbon, which confirms the oxazine ring formation. The peak appeared at 130ppm shows the presence of aliphatic -C=C- in the side chain indicates the existence of cardanol moiety in the newly synthesized benzoxazine monomer. In ^{13}C NMR, the peak visualized at 178ppm shows the presence of carbonyl carbon atoms and the peaks from 115 ppm to 145 ppm confirms the presence of aromatic carbon atoms. The peaks observed from 14 ppm to 42 ppm confirm the presence of aliphatic carbon atoms. Thus the ^{13}C NMR spectrum also confirms the formation of cardanol-based benzoxazine monomer.

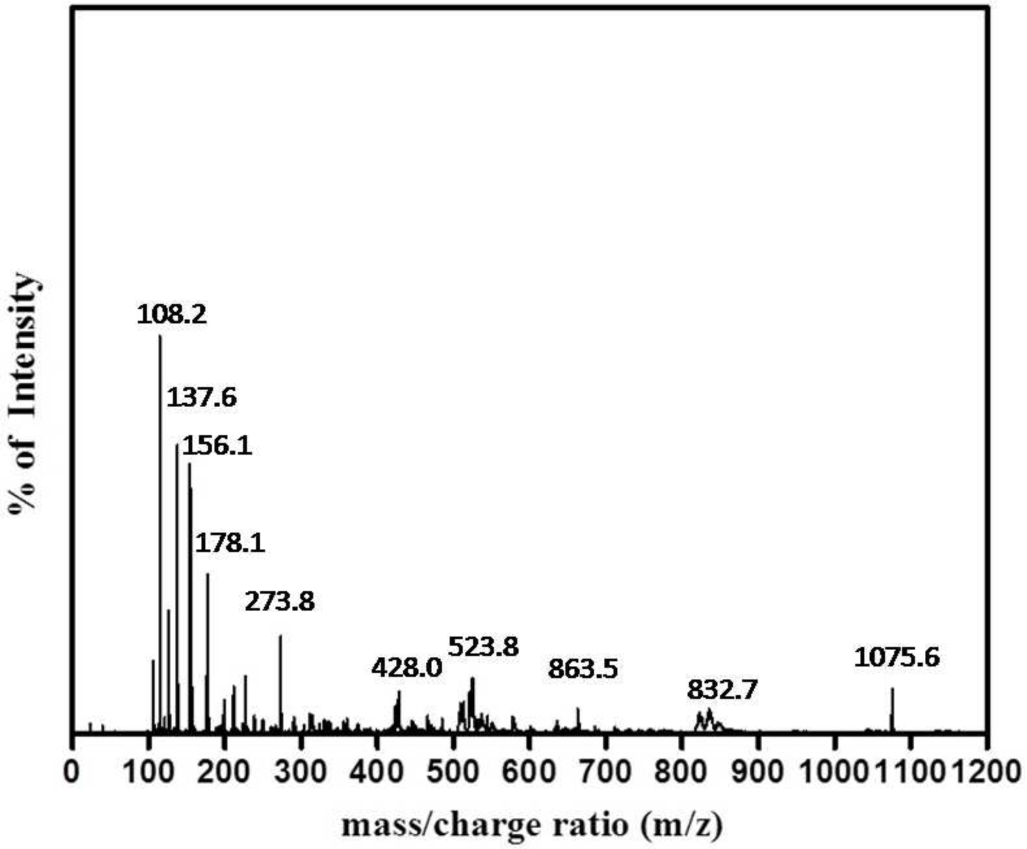

Figure 6b MALDI-Mass spectrum of cardanol benzoxazine (CBz)

MALDI –Mass analysis is an important technique used to determine the higher molecular weight of proteins, peptides, monomers and polymers etc. The formation as well as the molecular weight of cardanol based benzoxazine monomer is further confirmed by MALDI Mass spectroscopy (Figure 6b). The spectral analysis shows the molecular weight of the benzoxazine monomer as 1076, which is in good agreement with the theoretically calculated molecular weight value. Hence, the above results (^{1}H NMR, ^{13}C NMR and MALDI Mass) confirm the successful formation of cardanol based benzoxazine monomer.

Thermal Properties

DSC

The curing characteristic of a monomer was studied by DSC. The melting temperature, onset curing temperature, temperature of exothermic peak and heat of curing reaction were obtained from the DSC curve and their characteristic parameters were listed in Table 1.

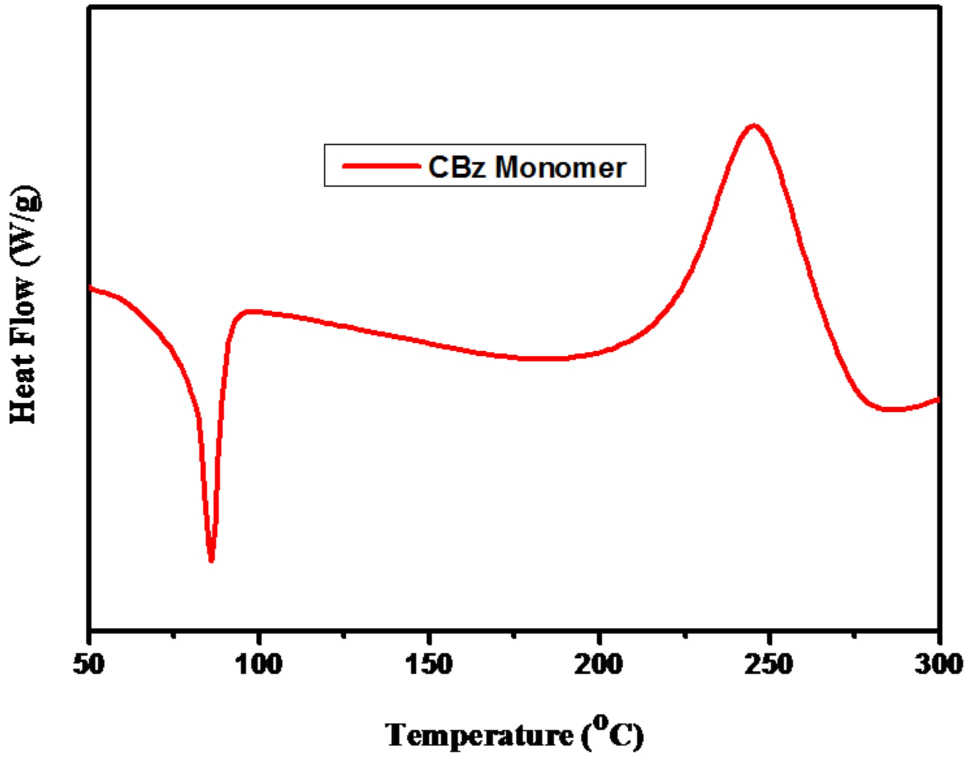

Figure 7 DSC of monomer cardanol benzoxazine

As seen in Figure 7, a sharp endothermic peak centered at 85.9^{0}C may be attributed to the melting point of CBz. The exothermic behavior observed at high temperature region was associated with the ring-opening polymerization of oxazine rings.

Table 1. Characteristic parameters of CBz

Parameters	Temperature (^{0}C)
Melting point	85.9
Onset cure temperature	220.8
Peak temperature	245.6
End temperature	271.4
Exothermic enthalpy(J/g)	150.3

The onset polymerization temperature of CBz has found to be 220.8^{0}C. The temperature difference between melting point and onset polymerization temperature for CBz is 134.9^{0}C, which indicates its good processing behavior. After initial polymerization, CBz may involve steric hindrance in polymerization due to the side long alkyl substituent, and shifted the exothermic peak to a high temperature of 245.6^{0}C. The reaction enthalpy of polymerization has found to be 150.3 J/g. The curing temperature of p-cresol based benzoxazine was 272^{0}C [27] and benzoxazine from cardanol-furfural resin was 275^{0}C[28]. These results illustrated that the curing temperature of the synthesized CBz was much lower than that of p-cresol based benzoxazine, which could be attributed to the presence of aliphatic bridging units of caprolactamdiamine into the cardanol based benzoxazine.

The glass transition temperature for neat PCBz and TSBA -15 (1, 3 and 5 wt %) reinforced nanocomposites were presented in Figure 8 and Table 2.

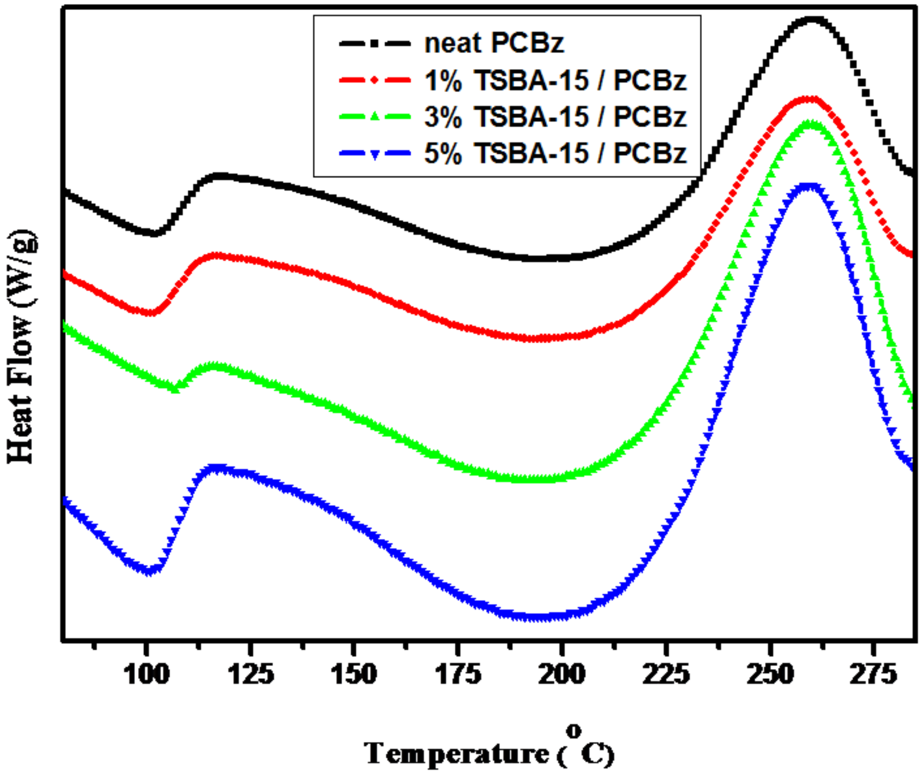

Figure 8 DSC thermograms of PCBz and TSBA-15/PCBz composites

From Table 2, it is clear that the Tg values of the TSBA-15/PCBz composites were increased with increasing the amount of TSBA-15 materials. The neat PCBz has a Tg value of 90.1^{0}C and incorporation of 5% TSBA-15 shifted the Tg value to 113.9^{0}C. The increase in value of Tg for TSBA-15/PCBz composite is due to restricted motion of bulky polybenzoxazine molecular chains, presence of long alkyl side chain of cardanol and also due to the incorporation of TSBA-15 material, which imparts rigidity.

TGA

The thermal stability of PCBz and TSBA-15/PCBz hybrids were evaluated by TGA and their results were listed in Table 2. Figure 9 shows the thermal stability of hybrid films and the 10%, 20% and 30% mass loss temperatures. All TSBA-15/PCBz composites showed similar decomposition curves of good thermal stability, which is due to the presence of long alkyl side chain of cardanol units in the polymer network. The char yield at 800^0 C for neat PCBz, 1% TSBA-15/PCBz, 3% TSBA-15/PCBz and 5% TSBA-15/PCBz were 12.24%, 14.05%, 17.26% and 18.98%, respectively.

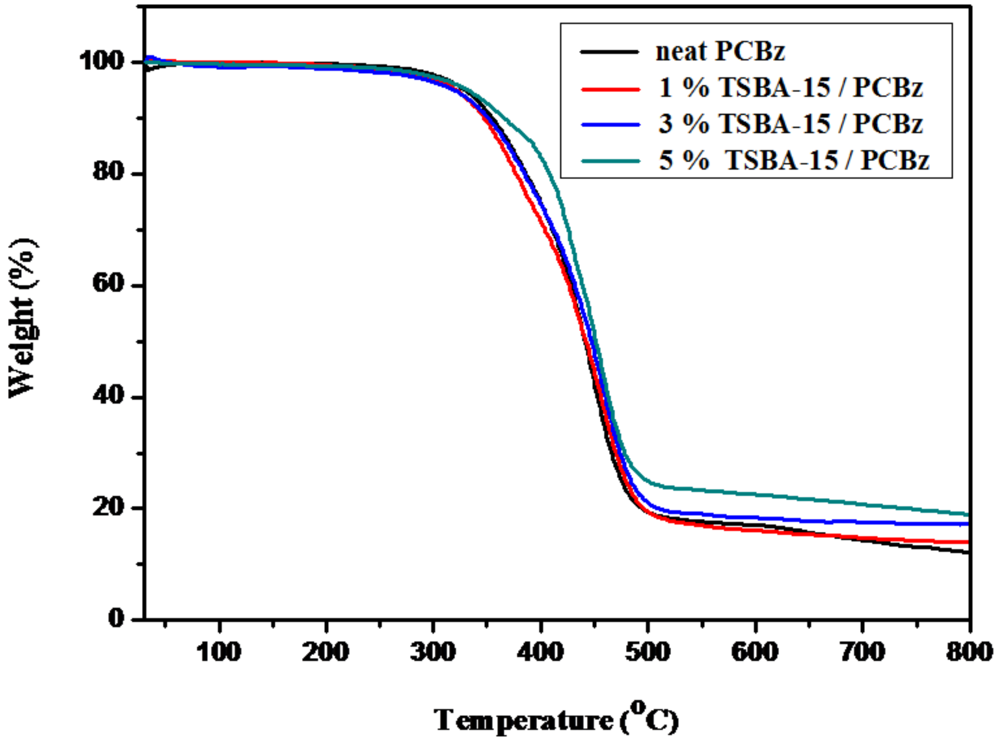

Figure 9 TGA thermogram of PCBz and various weight % of TSBA-15 in PCBz

The increasing char residue of hybrids resulted from the interaction of more inorganic TSBA-15 particles in the polybenzoxazine matrix. Further the nanofiller TSBA-15, which has high thermal stability and starts to decompose at higher temperature only. Thus TSBA-15 do not experience weight loss in the temperatures of 30-800°C. When the temperature was increased to 800°C, only the component of polybenzoxazine was almost decomposed. The incorporation of TSBA-15 increases the crosslinking density of the resulting nanocomposites and also restrict the chain mobility, which leads to an increase in the Tg values.

Table 2 Characteristic parameters from TGA, DSC and Dielectric Analysis

Sample	**Tg(°C)**	**T_{10}(°C)**	**T_{20}(°C)**	**T_{30}(°C)**	**Char yield % (800°C)**	**Dielectric constant at 1MHz**
Neat PCBz	90.1	348	378	405	12.24	3.52
1% TSBA-15 / PCBz	105.6	356	385	413	14.05	2.99
3% TSBA-15 / PCBz	109.4	361	394	422	17.26	2.32
5% TSBA-15 / PCBz	113.9	368	409	427	18.98	1.947

Dielectric properties

The dielectric constant of polymeric materials depends on the contribution of dipole, electronic and atomic polarization. For heterogeneous materials like composites, there is also possibility for interfacial polarization, which arises due to the differences in conductivities of the two phases. Figures 10 shows the frequency dependence of dielectric constant for PCBz and various weight % of TSBA-15 in PCBz and their results were shown in Table 2. From the Table 2, it is clear that the dielectric constant decreases with increasing the content of thiol modified SBA-15 material. Figure 11 shows the dielectric constant at 1MHz for PCBz and various weight % of TSBA-15 in PCBz. A similar type of observation (decreases with increasing TSBA-15 content) is also noticed for dielectric constant value at 1MHz (Figure 11). According to the previous report, the low k values (less than 2.5) can be achieved by the introduction of porosity since air has a dielectric constant close to unity [29,30]. Free volume is another important factor in determining the dielectric constant. The introduction of alkyl groups, flexible bridging units and bulky groups which limit chain packing density have been utilized to enhance free volume[31]. The presence of free volume in the form of pores will result in a decrease in dielectric constant as it is being occupied by air. The porosity can also be introduced in to the composites by inter-particulate voids formed between the particulates and the ordered pores arrangements formed in the solid by careful chemical design. Further, it has been known that the dielectric behavior of polymeric materials depend on the cross linking density, structure, and orientation relaxation of dipoles in the applied electric field. In addition to that the process of dipole polarization accompanies with the movement of polymer chain segments. Hence, in the present case with increasing the content of TSBA-15 can increase pores and voids at the micro scale level as evidenced from SEM and TEM images will affect the dielectric property of polymer composites significantly. Being a mesoporous material, the incorporation of TSBA-15 in to cardanol based benzoxazine matrix will create free space, which may be occupied by air of dielectric constant 1. The value of dielectric constant was decreased when the weight percentage of TSBA-15 is increased, due to the formation of air voids and pores. Figure 12 shows dielectric loss of the neat PCBz and various weight % of TSBA-15 incorporated PCBz. The presence of a strong bonded interface between TSBA-15 and PCBz may suppress the dielectric loss. The existence of effective interface interaction between TSBA-15 and PCBz may suppress the dielectric loss. The decrease in the values of dielectric constant and dielectric loss are also due to the formation of high cross linked network structure and inorganic –Si-O-Si–linkage due to its insignificant polarizability. The porosity or free volume also reduces polarizability, which inturn reduces the dielectric constant of the polymer composite[32,33]. The strong interaction of TSBA-15 with PCBz matrix is evidenced from SEM and the well-ordered arrangement of the composite with pores and voids could be visualized from TEM image. The mesoporous nature of TSBA-15 is also retained in the composites. Thus the presence of pores, voids and retained mesoporous nature of TSBA-15 in the composite material decreased the value of dielectric constant. The strong interfacial adhesion between filler and matrix leads to low dielectric loss. The low dielectric constant as well as low dielectric loss of the materials suggests that these materials can be used as an effective inter layer insulators in integrated circuitry devices for microelectronics applications.

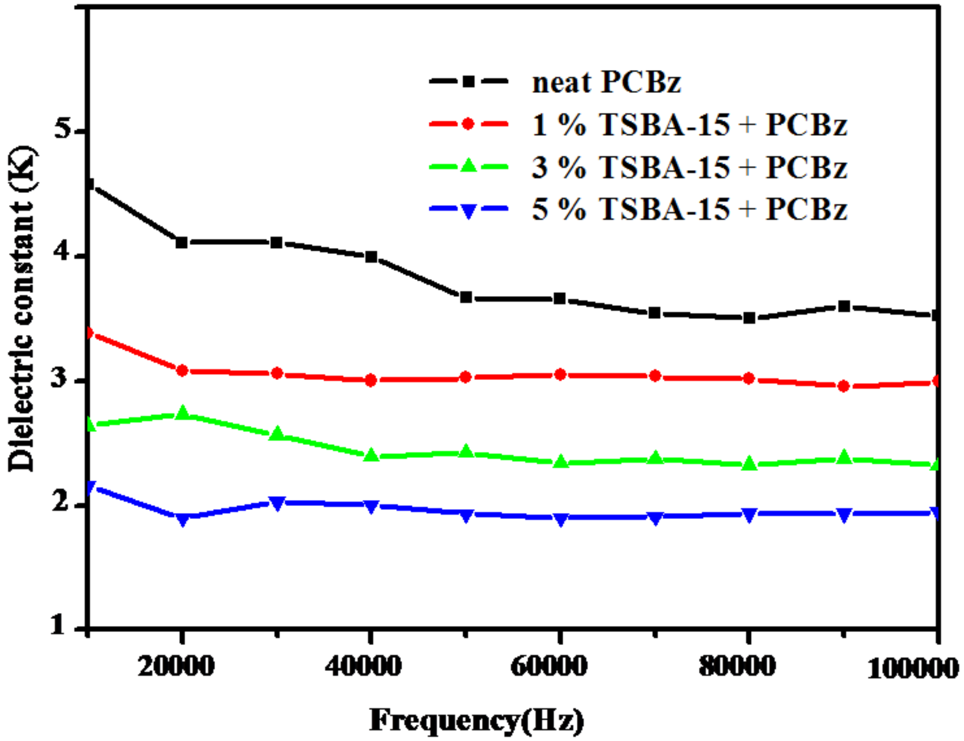

Figure 10 Dielectric constant of PCBz and various weight % of TSBA-15 in PCBz at varying frequencies.

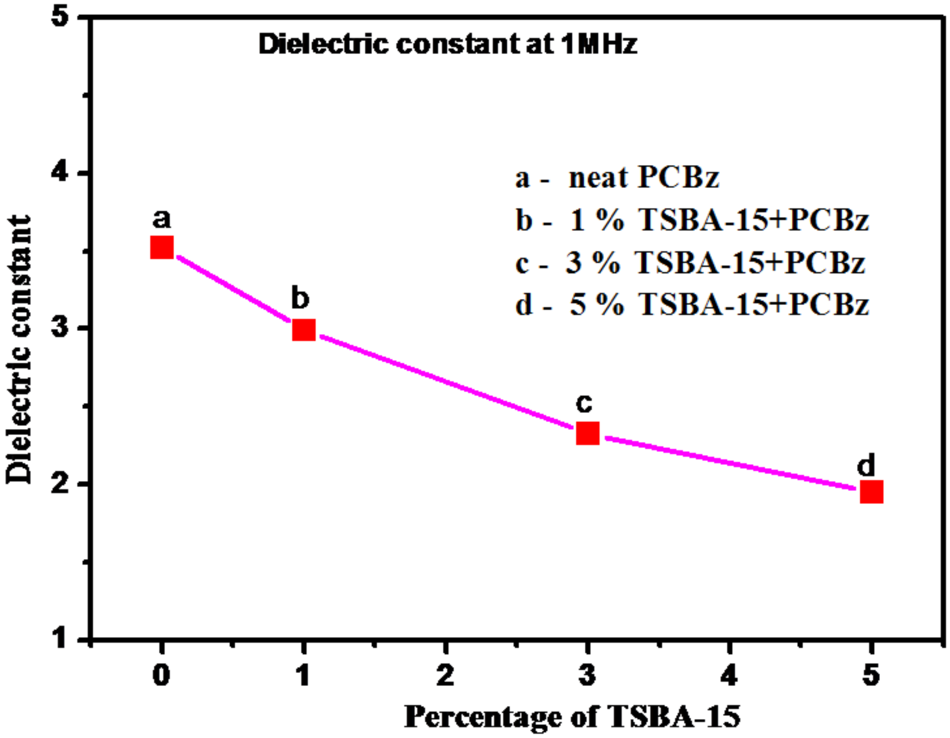

Figure 11 Dielectric constant of PCBz and various weight % of TSBA-15 in PCBz at 1MHz

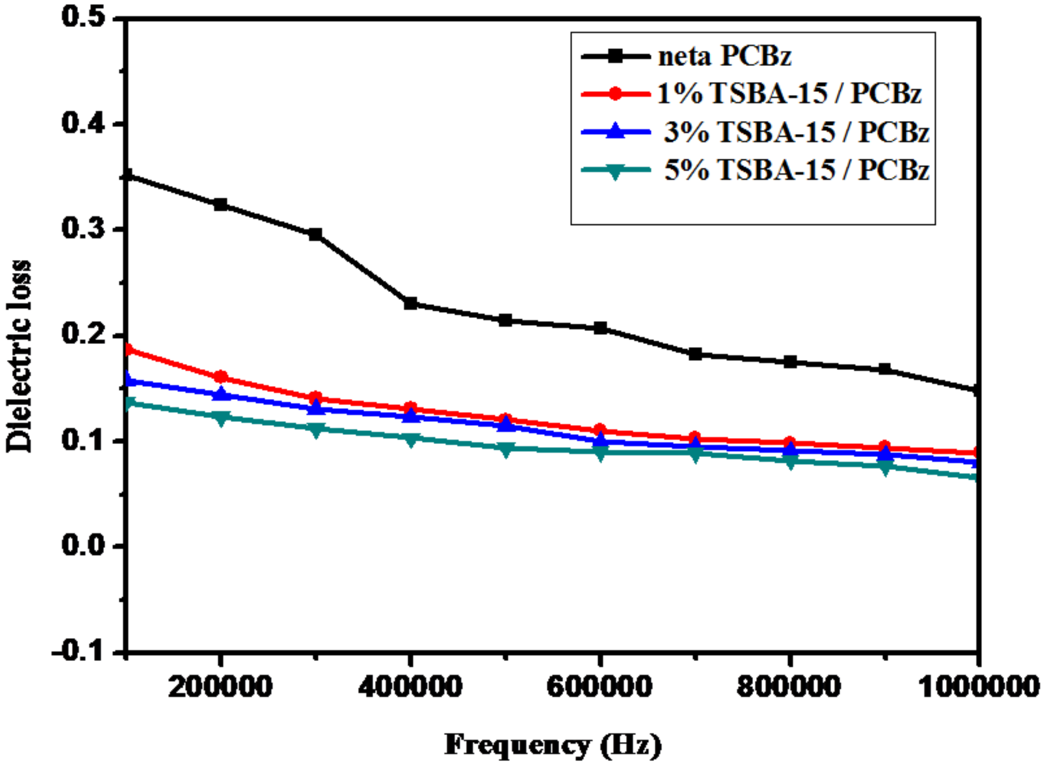

Figure 12 Dielectric Loss of PCBz and various weight % of TSBA-15 in PCBz.

XRD characteristics of PCBz/TSBA-15

The XRD patterns of TSBA-15 and TSBA-15 incorporated in PCBz were presented in Figure 13. The TSBA-15 showed peaks at 0.88 and 1.40 (2θ) for the silica planes (100) and (110), respectively. A decrease in the peak intensity was observed for the addition of different weight percentage of TSBA-15 to PCBz. Even though there is a decrease in peak intensity, there is only a slight change in peak position, which may be attributed to highly restricted mobility of polybenzoxazine, scattering contrast among the silica walls and pore channels.

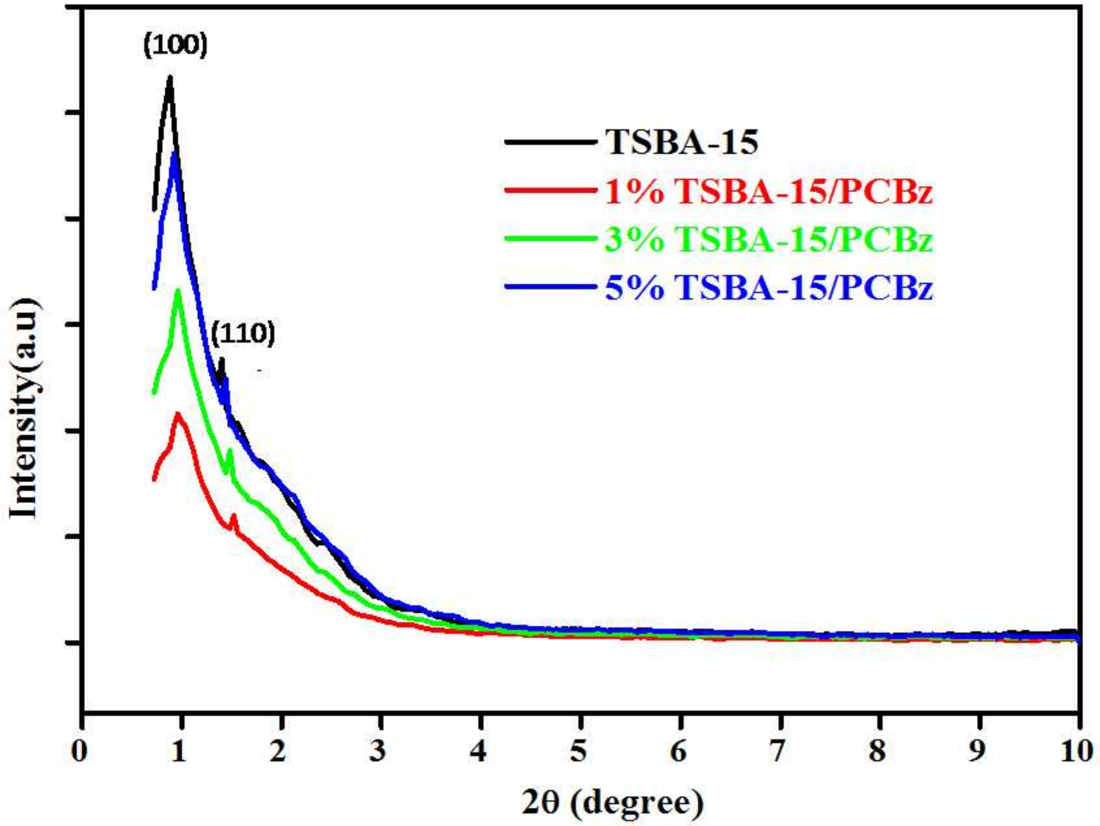

Figure 13 XRD patterns of TSBA-15 and PCBz/TSBA-15 composites

Morphological studies of PCBz and PCBz/ TSBA-15

The dark brown hybrid films were obtained by incorporating TSBA-15 in to PCBz and cured in a step wise manner. The morphologies of PCBz and TSBA-15/PCBz hybrid films were investigated by SEM (Figure 14). For PCBz, the surface of polymeric film was very smooth due to the single neat composition. When TSBA-15 is incorporated in to PCBz, the hybrid films became less smooth with formation of rope like domains of mesoporous silica [34] with cylindrical pores.

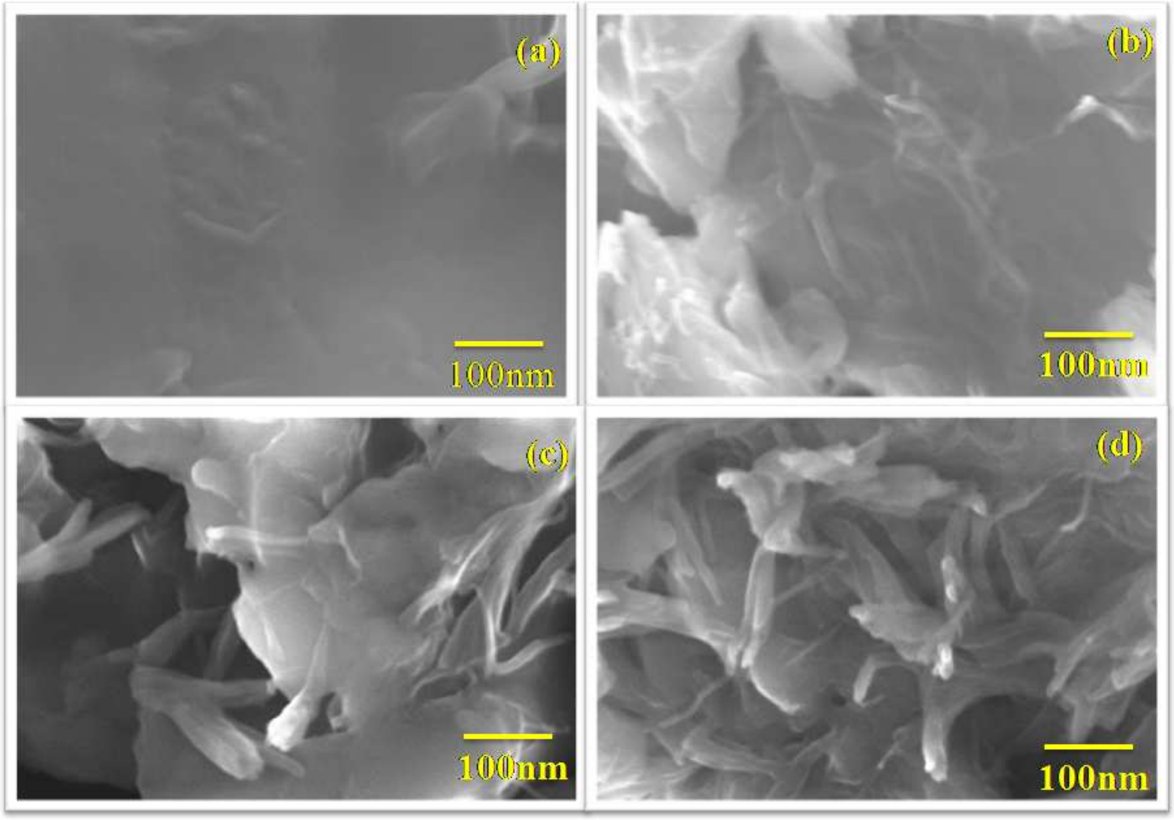

Figure 14 SEM micrograph of (a) Neat PCBz, (b) 1% TSBA-15/PCBz, (c) 3% TSBA-15/PCBz, (d) 5% TSBA-15/PCBz nanocomposites

TEM image (**Figure15**) shows the presence of TSBA-15 in the polybenzoxazine matrix as a chain like fibrous material. This is due to the introduction of thiol group in SBA-15 material using MPTMS and strong interfacial interactions resulted between the TSBA-15 and PCBz matrix. The long chain like structure with ordered cylindrical pores confirm a well-defined structure of TSBA-15/PCBz composite (Figure 15). This creates free volume, which lowers the dielectric constant significantly. From the TEM image, it has been visualized that the nanometer level dispersion of TSBA-15 in PCBz matrix, which could influence on the thermal and electrical properties of the resulting TSBA-15/PCBz nanocomposites.

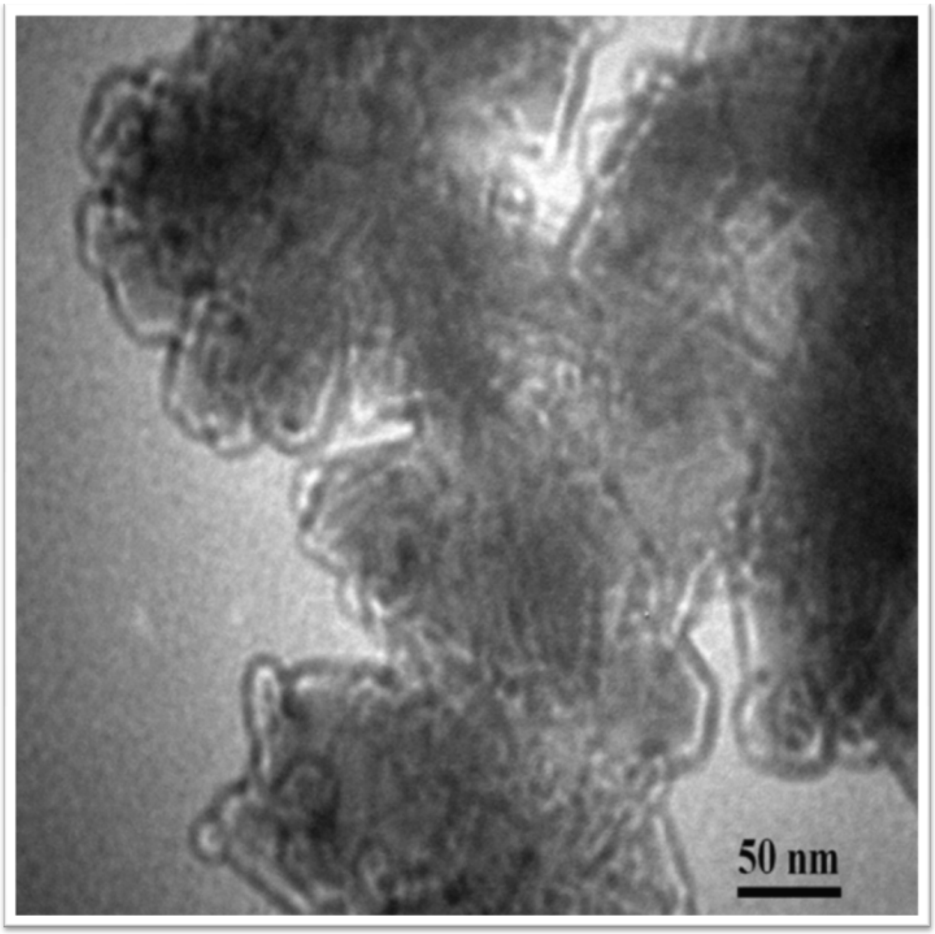

Figure 15 TEM micrograph of 5%TSBA-15/PCBz nanocomposite.

CONCLUSION

In the present work, a new approach has been made to apply waste to value technology by synthesizing a novel benzoxazine monomer from a renewable bio waste cardanol with a low curing temperature. TSBA-15 was used as an inorganic nanofiller and a hybrid composite of TSBA-15/PCBz materials were synthesized, which possess low dielectric constant and high thermal stability. The TEM image clearly shows the presence of long fibrous material, which imparts free volume. There is a significant improvement in glass transition temperature, dielectric constant, thermal stability and char yield. Thus these nanocomposites can be used as an advanced composite material in microelectronic engineering applications.

ACKNOWLEDGEMENTS

The authors would like to thank DST/Nanomission, New Delhi, India for financial support to carry out this work and establishment of Nanotech Research Lab through grant No. SR/NM/NS-05/2011(G). The authors also like to thank Dr.M.Mandhakini, Department of Nanoscience and Technology, ACTech, Chennai for the timely help and moral support and Mr. Satya Priya, Satya Cashew Chemicals Pvt. Ltd. Chennai for providing cardanol for research purpose.

References

1. S. F. Wang, T. R. Wang, K. C. Cheng and Y. P. Hsiao, *Ceramics International*, 2009, **35**, 265.
2. R. Tummala and E. J. Rymaszewski, *Microelectronics Packaging Handbook*, 1989, 1
3. S. Numata, K. Fujisaki, D Makino and N. Kinjo, *Society of Plastic Engineers, Inc*., 1985, 16
4. M. Ree, *Macromol. Res.*, 2006, **14**, 1.
5. H. Schreiber, *German Patent 2*, 1973, **255**, 504.
6. H. Schreiber, *German Patent* 2, 1973, **323** 936.
7. X. Ning and H. Ishida, *J. Polym. Sci. Part A: Polym. Chem.*, 1994, **32**, 1121
8. X. Ning and H. S. Ishida, *J. Polym. Sci. Part B: Polym. Phys.*, 1994, **32**, 921.
9. H. Ishida and D. J. Allen, *J. Polym. Sci. Part B: Polym Phys.*, 1996, **34**, 1019.
10. N. N. Ghosh, B. Kiskan and Y. Yagci, *Prog. Polym. Sci*., 2007, **32**, 1344.
11. S. Wirasate, S. Dhumrongvaraporn, D. J. Allen and H. Ishida, *J. Appl. Polym. Sci.* , 1998, **70**, 1299.
12. Y. C. Su and F. C. Chang, *Polymer*, 2003, **44**, 7989.
13. Y. C. Su, W. C. Chen, K. L. Ou and F.C. Chang, *Polymer*, 2005, **46**, 3758.
14. M. C. Tseng and Y. Liu , *Polymer*, 2010, **51**, 5567.
15. Y. W. Chen and E. T. Kang, *Mater. Lett.,* 2004, **58**, 3716.
16. C. M. Leu, Y. T. Chang and K. H. Wei , *Chem. Mater.*, 2003, **15**, 3721.
17. Q. R. Hung, W. Volksen, E. Huang, M. Toney, C.W. Frank and R. D. Miller, *Chem. Mater.*, 2002, **14**, 3676.
18. Q. R. Hung, H. C. Kim, E. Huang, D. Mecerreyes, J. L. Hedrick and W. Volksen, *Macromolecules*, 2003, **36**, 7661.
19. J. E. Mark, *Accounts of Chem.Res.*, 2006, **12**, 881.

20. E. Calo, A. Maffezzoli, G. Mele, F. Martina, S. E. Mazzetto, A. Tarzia, C. Stifani, *Green. Chem.*, 2007, **9**, 754.

21. B. Lochab, I. K. Varma and J. Bijwe, *J. Calorim. Anal. Therm.*, 2010, **102**, 769.

22. B. S. Rao and A. Palanisamy, *React. Funct. Polym.,* 2011, **74**, 148

23. J. Bijwe and P. V. Gurunath *PCT Int .Appl WO.,* 2008149380 A2 20081211, 2008.

24. J. Park, J. Park and H. Kim. *IPCBEE*, 2011, **24.**

25. K.Wilson, A.F.Lee, D.J.Macquarrie and J.H.Clark, *Appl.Catal.,A*, 2002, **228**, 127

26. V.Ganesan and A.Walcarius, *Langmuir*, 2004, **20**, 3632)

27. M. A. Espinosa, V. Ca´diz and M. Galia, *J. Appl. Polym. Sci*., 2003, **90**, 470.

28. S. F. Li, S. Yan, J. Yu and B. Yu, *J. Appl. Polym. Sci*., 2011, **122**, 2843.

29. B. D. Hatton, K. Landskron, W. J.Hunks, M. R. Bennett, D. Shukaris,D. Perovic, and G. A. Ozin, MaterialsToday, 2006, 9, 22.

30.S.-W. Kuo, F.-C. Chang / Progress in Polymer Science 36 ,2011, 1649–1696

31. G. Wypych, *Handbook of Fillers, 2nd Edition, Chemical Technology Publishing*, 1999, 2.

32.Y.S. Negi, Y. Suzuki, I.Kawamura, et.al., J. Polym. Sci. Part A: Polym. Chem., 30,1992,2281

33.Long, TM, Swager, TM, Journal of the American Chemical Society, 2003,125,1411-39

34. S. Ravi and M. Selvaraj, *Dalton Trans.*, 2014, **43**, 5299.

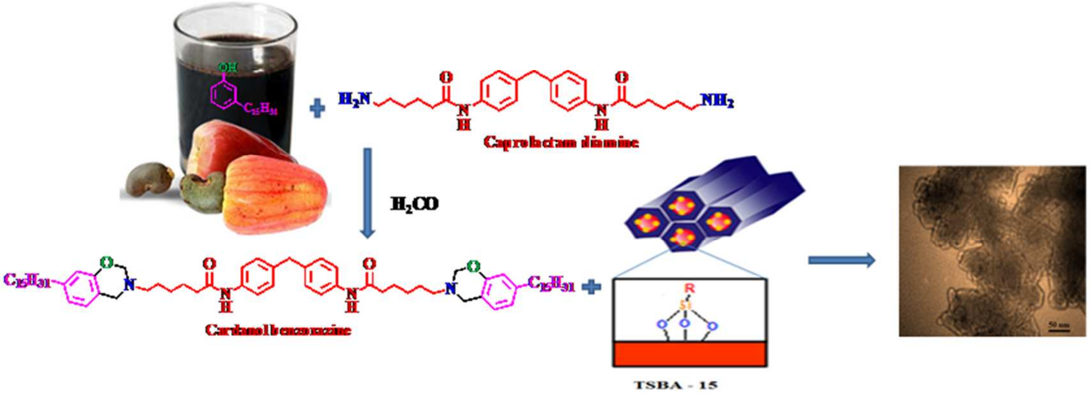

Scheme shows the synthesis of cardanol based polybenzoxazine composite for low Dielectric constant applications